Fibroblast growth factor 10 reverses cigarette smoke- and elastase-induced emphysema and pulmonary hypertension in mice

Stefan Hadzic[1], Cheng-Yu Wu[1], Marija Gredic[1], Oleg Pak[1], Edma Loku[1], Simone Kraut[1], Baktybek Kojonazarov[1,2], Jochen Wilhelm[1,2], Monika Brosien[1], Mariola Bednorz[1], Michael Seimetz[1], Andreas Günther[1], Djuro Kosanovic[1,3], Natascha Sommer[1], David Warburton[4,5], Xiaokun Li[6], Friedrich Grimminger[1], Hossein A. Ghofrani[1], Ralph T. Schermuly[1], Werner Seeger[1,7], Elie El Agha[1,2], Saverio Bellusci[8,9,10] and Norbert Weissmann[1,10]

[1]Excellence Cluster Cardio-Pulmonary Institute (CPI), Universities of Giessen and Marburg Lung Center (UGMLC), Member of the German Center for Lung Research (DZL), Justus-Liebig-University, Giessen, Germany. [2]Institute for Lung Health (ILH), Justus-Liebig-University, Giessen, Germany. [3]Sechenov First Moscow State Medical University (Sechenov University), Moscow, Russia. [4]Children's Hospital Los Angeles, Los Angeles, CA, USA. [5]Keck School of Medicine, University of Southern California, Los Angeles, CA, USA. [6]School of Pharmaceutical Sciences, Wenzhou Medical University, Wenzhou, P.R. China. [7]Max-Planck Institute for Heart and Lung Research, Bad Nauheim, Germany. [8]Oujiang Laboratory (Zheijiang Laboratory for Regenerative Medicine, Vision and Brain Health), School of Pharmaceutical Science, Wenzhou Medical University, Wenzhou, P.R. China. [9]Laboratory of Extracellular Matrix Remodelling, Excellence Cluster Cardio-Pulmonary Institute (CPI), Universities of Giessen and Marburg Lung Center (UGMLC), Member of the German Center for Lung Research (DZL), Justus-Liebig-University, Giessen, Germany. [10]S. Bellusci and N. Weissmann contributed equally to this article as lead authors and supervised the work.

Corresponding author: Norbert Weissmann (norbert.weissmann@innere.med.uni-giessen.de)

Shareable abstract (@ERSpublications)
Impaired FGF10 signalling is an integral part of the pathomechanism that leads to development of cigarette smoke-induced emphysema and PH. Restoration of FGF10 signalling reverses established cigarette smoke- and elastase-induced emphysema and PH in mice. https://bit.ly/3PgqrBw

Cite this article as: Hadzic S, Wu C-Y, Gredic M, *et al*. Fibroblast growth factor 10 reverses cigarette smoke- and elastase-induced emphysema and pulmonary hypertension in mice. *Eur Respir J* 2023; 62: 2201606 [DOI: 10.1183/13993003.01606-2022].

This article has an editorial commentary: https://doi.org/10.1183/13993003.01691-2023

Received: 16 Aug 2022
Accepted: 28 Aug 2023

Abstract

Background COPD is an incurable disease and a leading cause of death worldwide. In mice, fibroblast growth factor (FGF)10 is essential for lung morphogenesis, and in humans, polymorphisms in the human *FGF10* gene correlate with an increased susceptibility to develop COPD.

Methods We analysed FGF10 signalling in human lung sections and isolated cells from healthy donor, smoker and COPD lungs. The development of emphysema and PH was investigated in $Fgf10^{+/-}$ and $Fgfr2b^{+/-}$ (FGF receptor 2b) mice upon chronic exposure to cigarette smoke. In addition, we overexpressed FGF10 in mice following elastase- or cigarette smoke-induced emphysema and pulmonary hypertension (PH).

Results We found impaired FGF10 expression in human lung alveolar walls and in primary interstitial COPD lung fibroblasts. In contrast, FGF10 expression was increased in large pulmonary vessels in COPD lungs. Consequently, we identified impaired FGF10 signalling in alveolar walls as an integral part of the pathomechanism that leads to emphysema and PH development: mice with impaired FGF10 signalling ($Fgf10^{+/-}$ and $Fgfr2b^{+/-}$) spontaneously developed lung emphysema, PH and other typical pathomechanistic features that generally arise in response to cigarette smoke exposure.

Conclusion In a therapeutic approach, FGF10 overexpression successfully restored lung alveolar and vascular structure in mice with established cigarette smoke- and elastase-induced emphysema and PH. FGF10 treatment triggered an initial increase in the number of alveolar type 2 cells that gradually returned to the basal level when the FGF10-mediated repair process progressed. Therefore, the application of recombinant FGF10 or stimulation of the downstream signalling cascade might represent a novel therapeutic strategy in the future.

Introduction

COPD is a leading cause of morbidity and mortality worldwide, characterised by persistent airflow limitation due to chronic bronchitis and emphysema. The main risk factor contributing to COPD development is the inhalation of noxious particles or gases, particularly cigarette smoke and air pollution [1–3]. Structural remodelling of the pulmonary vasculature, which often accompanies COPD, leads to the development of pulmonary hypertension (PH) [4–7].

Emerging literature reports dysregulation of developmental pathways in lung emphysema, suggesting the importance of homeostatic mechanisms for lung structural integrity in adult life [3, 8–10]. Indeed, lung development, repair and homeostasis share several mechanisms and signalling pathways, including fibroblast growth factors (FGF) [3, 9–11]. However, complex interactions between master regulators of development and homeostasis in emphysema are still poorly understood [3].

Secreted, paracrine-acting FGFs regulate fundamental cellular processes such as proliferation, survival, migration, differentiation and metabolism [12]. FGF10 is indispensable for branching morphogenesis during embryonic lung development [13]. Mesenchyme-derived FGF10 predominantly binds to and activates its cognate receptor, FGFR2b, expressed by epithelial cells. Post-natally, FGF10/FGFR2b signalling regulates various aspects of stem/progenitor cell homeostasis, and activation in the lung promotes wound healing and prevents oxidant- and stretch-induced DNA damage in alveolar epithelial cells [14–19]. *FGF10* haploinsufficiency in humans has been linked to impaired lung function and single nuclear polymorphisms in the region of the *FGF10* locus were identified in COPD patients [11, 20, 21]. *Fgf10* mRNA expression was decreased in alveolar walls and increased in pulmonary vessels in cigarette smoke-exposed mice [6]. Selective inhibition of inducible nitric oxide synthase with L-N^6-(1-iminoethyl) lysine (L-NIL) successfully reversed established cigarette smoke-induced emphysema and PH [6]. Of interest, *Fgf10* upregulation positively correlated with L-NIL-mediated disease reversion [6]. However, the underlying mechanism remains largely elusive. Against this background, we aimed to investigate the role of FGF10 in the development and in treatment of lung emphysema and PH (supplementary figure S1).

Material and methods

Human lung tissue samples

Human lung tissue samples were obtained from the DZL Biobank, of individuals with and without COPD who had undergone lung transplantation or from healthy lung-transplantation donors. The pathologist examined all lungs and determined smoking status of the donors. Human serum was collected from donors and COPD patients with variable disease severity and PH status, following routine protocols. The ethics committee of the Justus-Liebig-University School of Medicine approved the studies (AZ 58/15; AZ 17/18).

Animal studies and experimental design

In the loss-of-function experimental setup (shown in supplementary figure S1a), mice that were haploinsufficient for either *Fgf10* or *Fgfr2b* (*Fgf10*$^{+/-}$ or *Fgfr2b*$^{+/-}$) were exposed to room air or cigarette smoke for 3 or 8 months (n=12 per group). Littermate mice with both functional *Fgf10* and *Fgfr2b* alleles were used as wild-type controls (n=12 per group). Furthermore, we overexpressed FGF10 in mice after cigarette smoke- or elastase-induced emphysema and PH (supplementary figure S1b). FGF10 overexpression was induced using doxycycline, using the Tet-ON system in transgenic B6-*Gt(ROSA)26Sor*$^{tm1.1(rtTA,EGFP)Nagy}$ Tg(*tetO-Fgf10*)*1Jaw/SpdlJ* mice (Jackson Laboratories, reference 025671). All animal lines were cross-bred to C57Bl/6J background. After 8 months of room air/cigarette smoke exposure, or 1 month after intratracheal saline/elastase instillation, animals were fed *ad libitum* with feed containing doxycycline (600 mg·kg^{-1}; Altromin Spezialfutter, Lage, Germany) for an additional 1, 5 or 12 weeks (n=12 animals per each group). The doxycycline-containing food was given for a week, followed by a week of "break", when mice were fed regular feed [15, 22]. In this way, animals could ingest high doses of doxycycline, but the common side-effects of long-term antibiotic treatment, or massive *Fgf10* overexpression, were minimised. Animals in control groups received feed lacking doxycycline. In previously published work, we demonstrated that doxycycline, given in such a way, does not affect cigarette smoke-induced emphysema and PH [22]. Before sacrificing, emphysema and PH phenotype in experimental mice was assessed *in vivo* by microcomputed tomography, echocardiography, lung function and haemodynamic measurements. In the case of *in vivo* measurements, n-numbers for final analysis vary due to technical reasons (*e.g.* animal death during measurements, incorrect placement of the haemodynamic catheter or the echocardiographic transducer or unsuccessful lung fixation). All animal experiments were approved by the local governmental authorities (Regierungspräsidium Gießen) in accordance with the German animal welfare law and the European legislation for the protection of animals used for scientific purposes (2010/63/EU).

Information about all other methods used in this study can be found in the supplementary material.

Results

FGF10 signalling is impaired in the lungs of individuals with COPD

FGF10 expression was significantly downregulated in alveolar walls and upregulated in vessels of lungs explanted from human subjects with end-stage emphysema (figure 1a). Upregulation of FGF10 was limited to the smooth muscle cell layer of the muscularised proximal pulmonary vessels, whereas no change could be observed in smaller distal vessels (supplementary figure S2a). FGF10 levels in the serum of COPD patients were lower compared to healthy donors and were independent of the Global Initiative for Chronic Obstructive Lung Disease stage or diagnosed pulmonary hypertension (supplementary figure S2b). Slight downregulation of FGF10 in alveolar walls of smokers without emphysema was accompanied by increased expression of FGFR2 (figure 1b), which might explain the absence of emphysema. Moreover, FGF10 levels in alveolar septa negatively correlated with emphysema severity in COPD lungs (supplementary figure S2c).

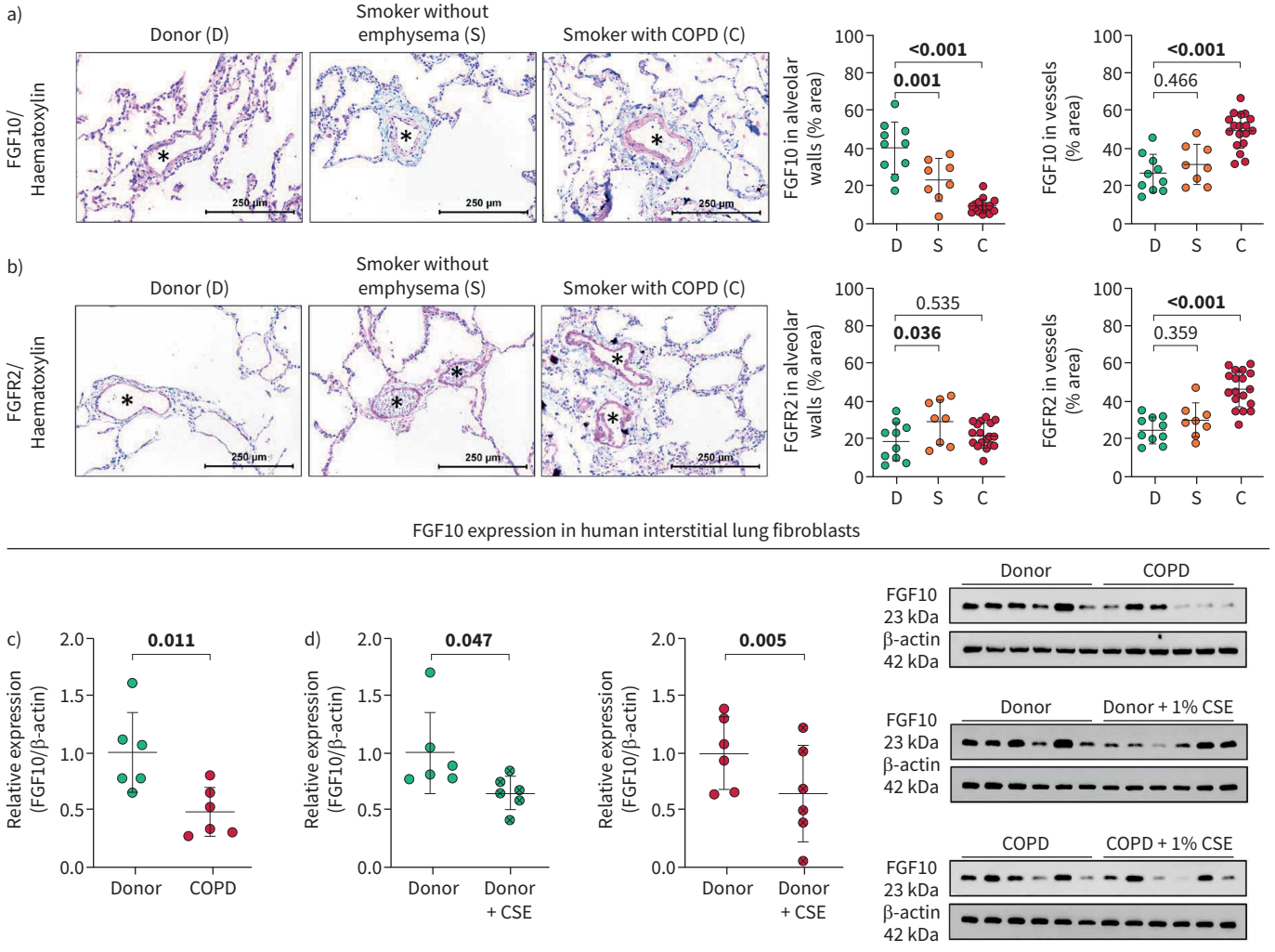

FIGURE 1 Fibroblast growth factor (FGF)10 signalling in human donor and COPD lungs. a, b) Representative images and quantification of a) FGF10 and b) FGFR2 staining in human lung sections from healthy donors (D; n=10), smokers without emphysema (S; n=8) and smokers with COPD (C; n=18). Asterisks (*) indicate pulmonary vessels. c, d) FGF10 expression quantified by Western blotting in lung interstitial fibroblasts isolated from c) healthy donor lungs (n=6) and COPD lungs (n=6); d) healthy donor (n=6) and COPD (n=6) lungs *in vitro* treated with cigarette smoke extract (CSE). Protein expression in Western blot was quantified by band densitometry analysis and standardised to β-actin; relative expression was calculated by standardising each value to the mean value of the corresponding control group. Immunohistochemistry: red: FGF10/FGFR2; blue: haematoxylin. In the quantification panels each dot represents a measurement obtained from an individual COPD or healthy donor. The mean value for each group is represented by a horizontal line (±SD). Statistical analysis: a, b) one-way ANOVA (Dunnett's multiple-to-one comparison); c) unpaired and d) paired t-test; p-value for each comparison is given in the graphs. Bold type represents statistical significance.

Next, we investigated FGF10 expression *in vitro* in interstitial fibroblasts isolated from lungs explanted from healthy donors and people with end-stage emphysema. Interestingly, FGF10 expression remained impaired in COPD fibroblasts compared to donors, despite the *in vitro* propagation of the cells (figure 1c). Furthermore, cigarette smoke extract (CSE) treatment *in vitro* decreased FGF10 expression in interstitial lung fibroblasts isolated from healthy donors and from individuals with COPD (figure 1d).

Mice with impaired FGF10 signalling spontaneously develop PH and emphysema

To decipher the role of the FGF10/FGFR2b signalling axis during emphysema development, we exposed *Fgf10*$^{+/-}$ and *Fgfr2b*$^{+/-}$ mice along with wild-type littermates to cigarette smoke for 3 or 8 months (supplementary figure S3a). FGF10 was downregulated in lung homogenates from cigarette smoke-exposed mice. FGF10 expression in lungs of room air-exposed *Fgf10*$^{+/-}$ mice was at a similar level as in cigarette smoke-exposed wild-type animals and, interestingly, did not further decrease upon cigarette smoke exposure (supplementary figure S3b–d).

At the 3-month time point, wild-type and *Fgf10*$^{+/-}$ had a similar increase in right ventricular systolic pressure (RVSP) upon cigarette smoke exposure (figure 2a). *Fgfr2b*$^{+/-}$mice had increased RVSP compared to the corresponding wild-type controls, which could be due to a slight increase in systemic arterial pressure (supplementary figure S4a). Our transgenic animals developed PH with ageing (8-month time point). The pressure measurements were consistent with the heart function data obtained by echocardiography (decreased tricuspid annular plane systolic excursion (TAPSE)) and right ventricular (RV) hypertrophy (figure 2b and c). Notably, we observed lower vessel density in room air-exposed *Fgf10*$^{+/-}$ and *Fgfr2b*$^{+/-}$ mice (figure 2d). Vascular pruning is indeed described in smokers' lungs [23], whereas FGF10 is known to stimulate vasculogenesis and angiogenesis [24]. Cigarette smoke exposure could thus lead to vascular pruning, remodelling and PH *via* FGF10 downregulation. Moreover, cigarette smoke-exposed mice and mice with impaired FGF10 signalling exhibited pronounced vascular remodelling, measured as an increase in muscularisation of usually nonmuscularised or slightly muscularised pulmonary vessels confirming haemodynamic data (figure 2e, supplementary figure S4b). These results support the hypothesis that FGF10 signalling in the pulmonary vasculature plays an important protective role rather than contributing to pulmonary vascular remodelling [25].

As reported previously, 3 months of cigarette smoke exposure in mice is sufficient to induce significant alterations in the pulmonary vasculature, while 8 months is needed for emphysema development [5, 6, 22, 26]. *Fgf10*$^{+/-}$ and *Fgfr2b*$^{+/-}$ mice developed emphysema much earlier than their wild-type littermates: after only 3 months of cigarette smoke exposure. Intriguingly, at the 8-month time point, room air-exposed *Fgf10*$^{+/-}$ and *Fgfr2b*$^{+/-}$ mice developed emphysema spontaneously, seen as significantly increased airspace percentage (figure 3a and b), increased mean linear intercept (MLI), decreased alveolar wall thickness and increased air-to-tissue volume ratio, compared to the room air-exposed wild-type controls (supplementary figure S5a–c). These findings were also confirmed using design-based stereology (figure 3c). Furthermore, mice with impaired FGF10 signalling showed significantly higher cellular senescence and spontaneously developed other typical pathomechanistic features that generally arise in response to cigarette smoke exposure (supplementary material, supplementary figures S5e–g and S6–8).

In vivo fluorescence molecular tomography–computed tomography measurements revealed increased matrix metalloproteinase (MMP) activity and apoptosis (figure 3d, supplementary figure S9a) in cigarette smoke-exposed wild-type animals and room air-exposed mice with impaired FGF10 signalling (*Fgf10*$^{+/-}$ and *Fgfr2b*$^{+/-}$) mice at the 3- and 8-month time points with spontaneous emphysema. FGF10 expression in fibroblasts is hypothesised to affect adjacent alveolar epithelial type 2 (AT2) cells during emphysema formation. Indeed, *in vitro* pre-treatment with recombinant FGF10 was able to prevent CSE-induced apoptosis and decreased viability in isolated AT2 cells (supplementary figure S9b).

FGF10 overexpression reverses cigarette smoke-induced PH and emphysema

We then tested whether FGF10 overexpression is sufficient to drive lung repair and reverse established cigarette smoke-induced emphysema and PH (supplementary figure S10a). We confirmed FGF10 overexpression *via* Western blotting and immunostaining in the lungs of animals fed with doxycycline (supplementary figure S10b and c). Between the examined groups, we could not detect changes in FGFR2 expression levels (supplementary figure S10d). Cigarette smoke-exposed mice developed PH and emphysema that remained stable for up to 3 months upon cigarette smoke cessation. FGF10 overexpression for 5 weeks was sufficient to completely reverse the cigarette smoke-induced increase of RVSP and RV hypertrophy and the decrease of RV function (figure 4a–c, supplementary figure S11a and b). Reversal of PH in FGF10-treated animals was associated with the reduction of cigarette smoke-induced remodelling (muscularisation) of small pulmonary vessels (figure 4d, supplementary figure S11c).

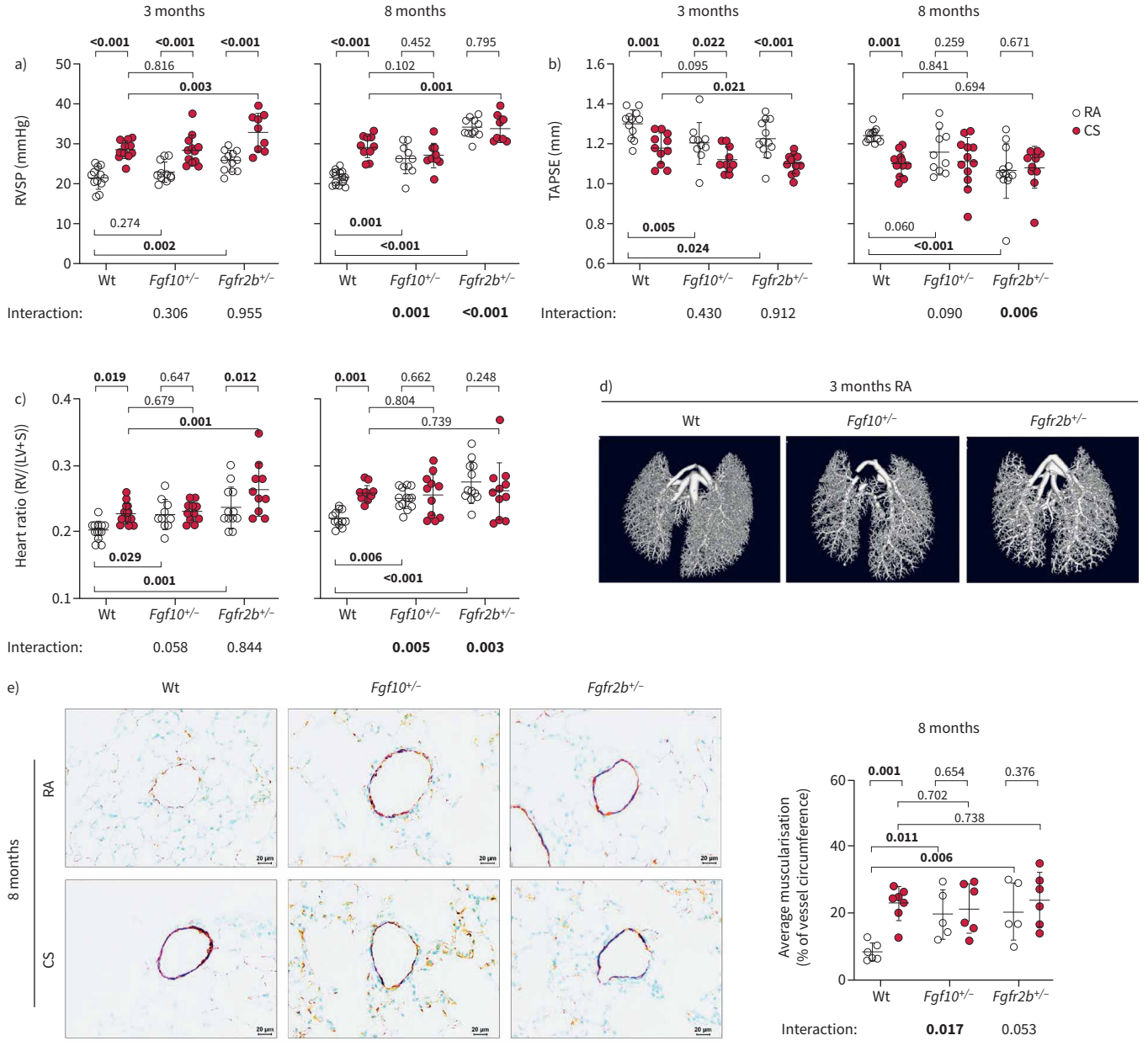

FIGURE 2 Mice with impaired fibroblast growth factor (FGF)10 signalling spontaneously develop pulmonary hypertension. Pulmonary hypertension assessed by measurement of a) right ventricular systolic pressure (RVSP) (n=9–12) and b) echocardiographic tricuspid annular plane systolic excursion (TAPSE) quantification (n=10–12). c) Right ventricular (RV) hypertrophy quantified by the weight ratio between the RV and left ventricle with septum (LV+S) (n=10–12). No significant changes in LV+S mass were detected between analysed groups. d) Pulmonary vasculature visualised *ex vivo* by microcomputed tomography in lungs perfused with radio-dense Microfil, representative scans of lungs from wild-type (Wt), *Fgf10*$^{+/-}$ or *Fgfr2b*$^{+/-}$ mice exposed to room air (RA) for 3 months. e) Representative images of pulmonary vessels (brown: von Willebrand factor; purple: α-smooth muscle actin; green: nuclei) and quantification of average vessel muscularisation in lungs of experimental animals (n=5–7). Analysis was performed in pulmonary vessels with a diameter of 20–70 µm and results are shown as percentage of vessel circumference positive for α-smooth muscle actin staining. In the quantification panels each dot represents a measurement obtained from one individual experimental animal. The mean value for each group is represented by a horizontal line (±SD). Statistical analysis: two-way ANOVA; p-values for each comparison and interaction are given in the graphs. CS: cigarette smoke. Bold type represents statistical significance.

Intriguingly, FGF10 overexpression successfully reversed established cigarette smoke-induced emphysema as demonstrated by the increase of alveolar numbers, decrease in MLI (figure 5a and b), decrease in airspace percentage and increase in alveolar wall thickness (supplementary figure S11d). The number of proliferating (Ki67^{+}) cells was increased in mouse lungs upon FGF10 treatment (supplementary figure S11e). AT2 cell

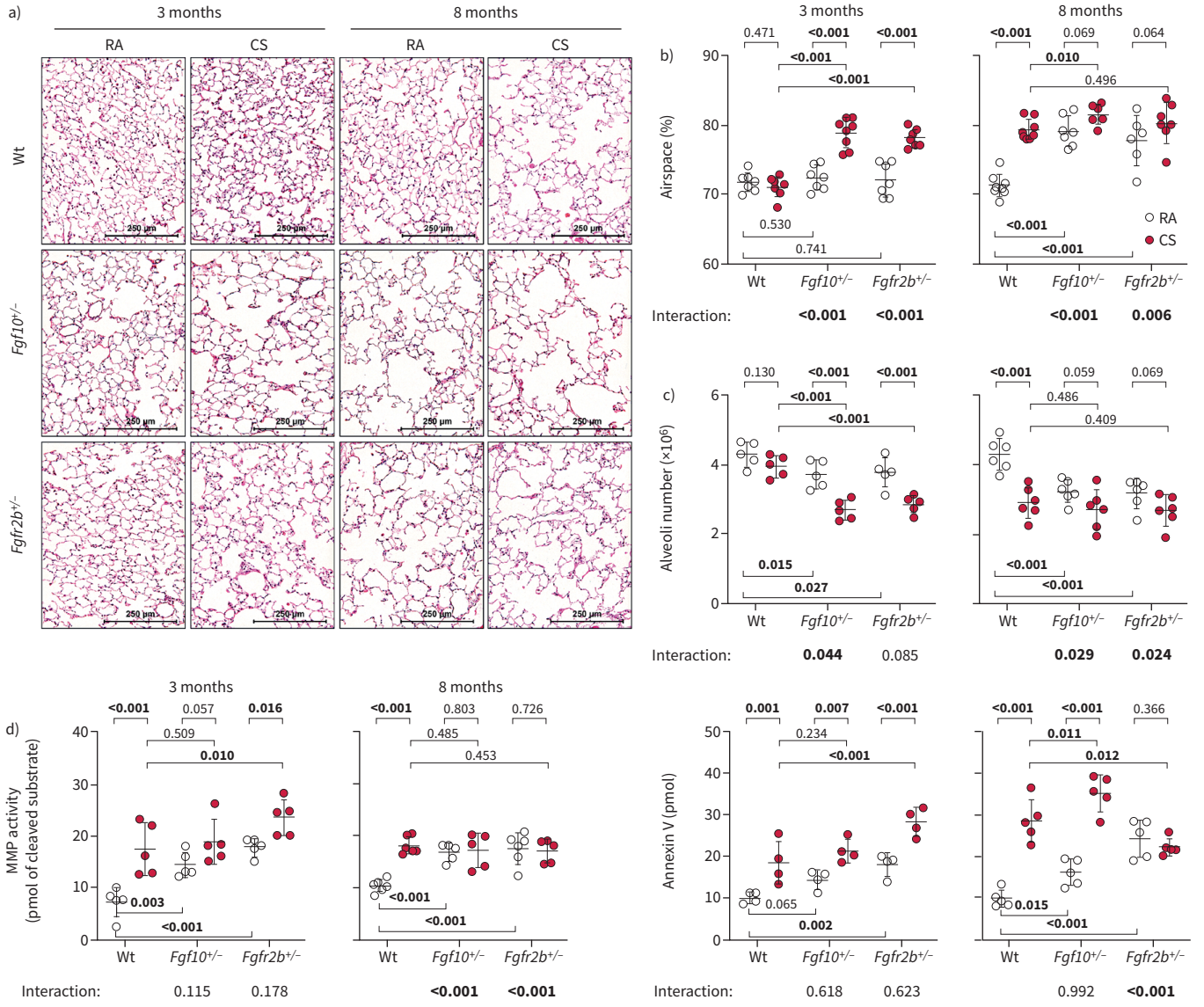

FIGURE 3 Mice with impaired fibroblast growth factor (FGF)10 signalling spontaneously develop pulmonary emphysema. a) Representative images of haematoxylin and eosin-stained lung sections of wild-type (Wt), *Fgf10*$^{+/-}$ or *Fgfr2b*$^{+/-}$ mice exposed to cigarette smoke (CS) or room air (RA) for 3 or 8 months. b, c) Pulmonary emphysema was quantified by determination of b) airspace percentage quantified using histological analysis (n=6–8) and c) alveoli number from left lung lobes using design-based stereology (n=5–6). d) *In vivo* matrix metalloproteinases (MMP) activity (MMPsense probe representing activity of MMP 2, 3, 7, 9, 12 and 13) or apoptosis (Annexin-Vivo probe) assessed using fluorescence molecular tomography imaging in experimental animals (n=4–6). In the quantification panels each dot represents a measurement obtained from one individual experimental animal. The mean value for each group is represented by a horizontal line (±SD). Statistical analysis: a–c) two-way ANOVA; d) paired two-way ANOVA; p-values for each comparison and interaction are given in the graphs. Bold type represents statistical significance.

number in the distal lung parenchyma and gene expression of epithelial progenitor markers (*Scgb1a1* and *Sftpc*) in bronchi were significantly increased in cigarette smoke-exposed mice upon FGF10 treatment for 1 week (figure 5c and d). The AT2 cell counts returned to the physiological level (figure 5c), while the area covered by AT1 cells increased (supplementary figure S11f) as lung structure was restored. Our results thus indicate that emphysema reversion could be mediated *via* the FGF10 effect on epithelial progenitor cells. Moreover, in the lung sections of cigarette smoke-exposed mice, we observed a significantly decreased von Willebrand factor immunostaining compared to room air-exposed controls, indicating loss of vessels. The cigarette smoke-induced decrease in von Willebrand factor staining was reversed by FGF10 overexpression (figure 5e). Additionally, FGF10 overexpression affected the composition of the extracellular matrix and reversed cigarette smoke-induced collagen accumulation in alveolar septa (supplementary figure S12).

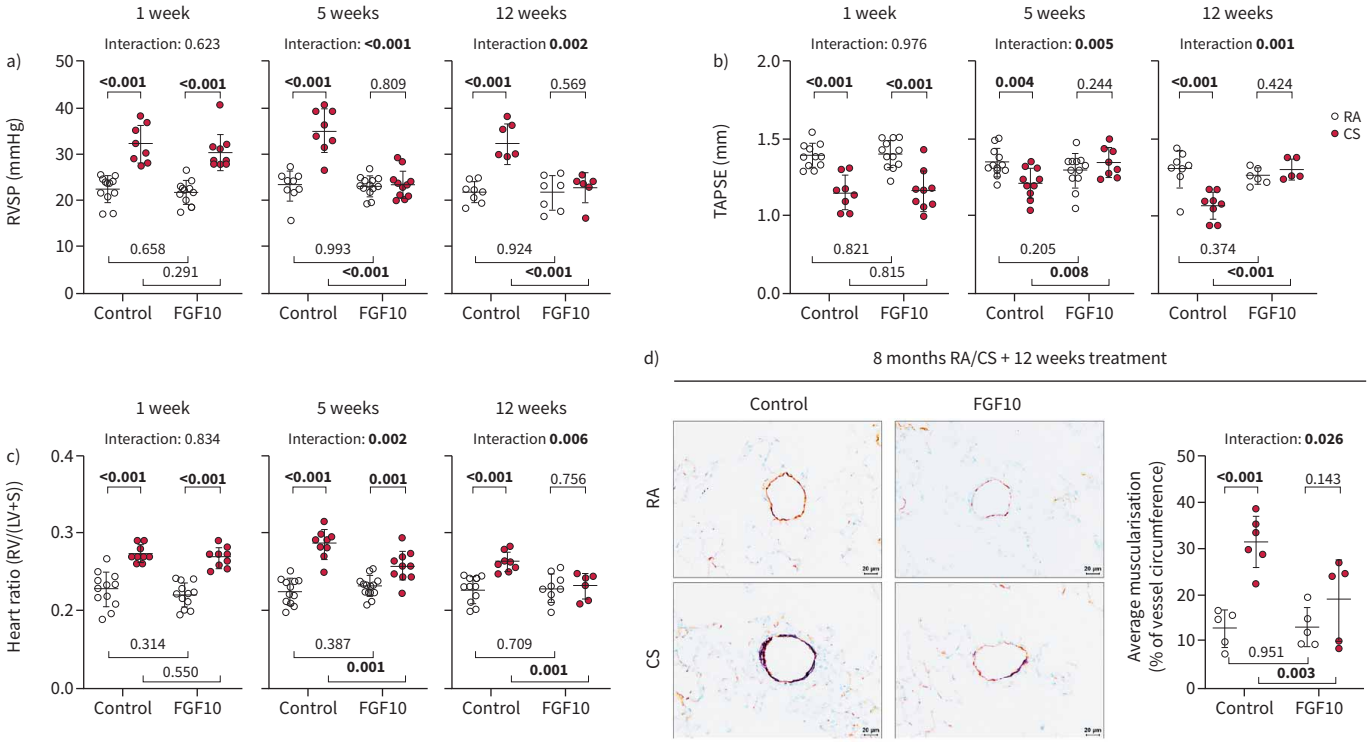

FIGURE 4 Fibroblast growth factor (FGF)10 overexpression reverses cigarette smoke (CS)-induced pulmonary hypertension in mice. a) Right ventricular systolic pressure (RVSP) (n=6–12), b) tricuspid annular plane systolic excursion (TAPSE) (n=5–12) and c) weight ratio of right ventricle (RV) and left ventricle plus septum (LV+S) (n=6–12), measured in CS- or room air (RA)-exposed mice that were subsequently fed with standard feed (control) or feed containing doxycycline (FGF10) for 1, 5 or 12 weeks. No significant changes in LV+S mass were detected between analysed groups. d) Representative images of pulmonary vessels (brown: von Willebrand factor; purple: α-smooth muscle actin; green: nuclei) and quantification of average vessel muscularisation in lungs of experimental animals (n=5–6). Analysis was performed in pulmonary vessels with a diameter of 20–70 µm and results are shown as percentage of vessel circumference positive for α-smooth muscle actin staining. In the quantification panels each dot represents a measurement obtained from one individual experimental animal. The mean value for each group is represented by a horizontal line (±SD). Statistical analysis: two-way ANOVA; p-values for each comparison and interaction are given in the graph. Bold type represents statistical significance.

Fgf10$^{+/-}$ mice have a similar gene expression pattern to cigarette smoke-exposed wild-type mice

To decipher the underlying mechanisms of emphysema and PH development, we analysed gene expression profiles in wild-type and *Fgf10*$^{+/-}$ animals at a 3-month time point. We used laser-assisted microdissection to separately collect RNA from alveolar walls and pulmonary vessels of the experimental mouse lungs. Gene expression analysis was then performed using microarrays. We observed a strong correlation between general gene expression patterns of wild-type cigarette smoke and *Fgf10*$^{+/-}$ room air, compared with wild-type room air control (supplementary figure S13). Further analysis revealed 263 genes in the alveolar walls and 289 genes in pulmonary vessels that are commonly regulated between wild-type cigarette smoke and *Fgf10*$^{+/-}$ room air, compared with wild-type room air control (figure 6a). Moreover, in both compartments, these genes were regulated in the same direction (figure 6b) and, largely, not further changed upon cigarette smoke exposure in *Fgf10*$^{+/-}$ mice (supplementary figure S13a–d). Of importance, these findings indicate that the transcriptomic alterations occurring in response to cigarette smoke exposure are already "saturated" in the context of *Fgf10* loss of function and that altered FGF10/FGFR2b seems to be central to the pathogenesis of cigarette smoke-induced PH and emphysema.

Genes involved in the FGF10-mediated reversal of cigarette smoke-induced emphysema and PH were analysed at the earliest time point: 1 week of FGF10 overexpression after 8 months of cigarette smoke exposure. In the alveolar wall compartment, we found 209 genes that were affected by both cigarette smoke exposure and subsequent FGF10 overexpression. In the pulmonary vasculature, 153 genes were commonly regulated (figure 6a). The vast majority of genes in the alveolar wall compartment were inversely regulated upon FGF10 overexpression compared to cigarette smoke exposure (figure 6b, supplementary figure S13e–h). Furthermore, endothelial nitric oxide synthase (*Nos3*) was downregulated in

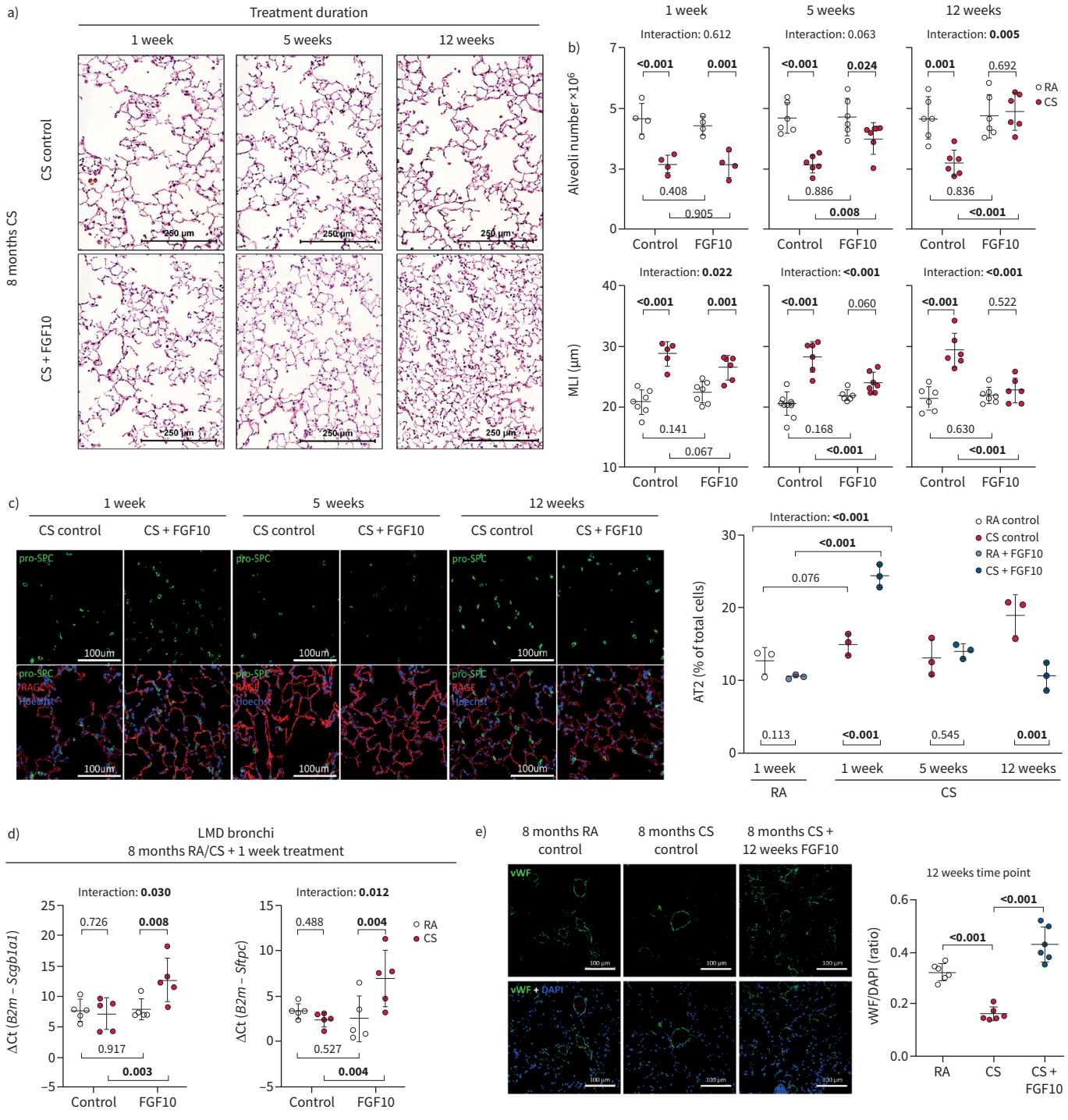

FIGURE 5 Fibroblast growth factor (FGF)10 overexpression reverses cigarette smoke (CS)-induced pulmonary emphysema in mice. a) Representative images of haematoxylin and eosin stained lung sections from the respective experimental groups. b) Pulmonary emphysema was histologically quantified in CS- or room air (RA)-exposed mice that were subsequently fed with standard feed (control) or feed containing doxycycline (FGF10) for 1, 5 or 12 weeks, shown as alveoli number (calculated by design-based stereology, n=4–6) or mean linear intercept (MLI) (n=5–7). c) Immunofluorescence staining for alveolar epithelial type 2 cells (AT2, pro-surfactant protein C (pro-SPC)) and type 1 cells (receptor for advanced glycation end products (RAGE)) in lungs of experimental animals. Quantification shows percentage of AT2 of total lung cells in distal lung parenchyma (n=3). No significant changes in nuclei count were detected between analysed groups. d) mRNA expression of epithelial progenitor markers (secretoglobin family 1A member 1 (*Scgb1a1*) and surfactant protein C (*Sftpc*)) in laser microdissected bronchi of experimental mice (n=5). mRNA was quantified using reverse transcriptase quantitative PCR and expression of the gene of interest related to the expression of *B2m* used as a reference gene. e) Immunofluorescence staining and fluorescence intensity quantification of von Willebrand factor (vWF)/4′,6-diamidino-2-phenylindole (DAPI) in lungs from CS-treated mice with or without doxycycline-induced FGF10 overexpression for 12 weeks (n=6). In the

quantification panels each dot represents a measurement obtained from one individual experimental animal. The mean value for each group is represented by a horizontal line (±SD). Statistical analysis: two-way ANOVA; p-values for each comparison and interaction are given in the graphs. Bold type represents statistical significance.

alveolar walls upon cigarette smoke exposure and upregulated with FGF10 overexpression. This suggests that the endothelium in the alveolar walls could be affected by cigarette smoke exposure and by FGF10 overexpression, as previously shown in figure 5e.

However, in the pulmonary vasculature, we could distinguish two populations of genes (figure 6b). One group of genes was inversely regulated by FGF10 expression compared to the effect of cigarette smoke exposure. These genes could be involved in the reverse remodelling process and resolution of cigarette smoke-induced PH. We found transcription factor TOX high mobility group box family member 2 (*Tox2*) that could be of interest for the mechanism of PH reversion. *Tox2* was the most prominently downregulated gene in the pulmonary vasculature upon cigarette smoke exposure and markedly upregulated with FGF10 overexpression. Interestingly, single-nucleotide polymorphisms in the human *TOX2* gene were associated with increased diastolic blood pressure in systemic circulation [27]. In pulmonary vasculature, the other group of genes was regulated in the same direction by cigarette smoke exposure and FGF10 overexpression. This finding is not surprising, considering that cigarette smoke exposure also upregulates FGF10 in the pulmonary vascular compartment.

The gene regulation pattern and the genes with the most robust regulation are depicted in heat maps (supplementary figure S14). In order to identify pathways and test if the regulated genes align in specific signalling pathways, we performed functional protein association network analysis (STRING-DB) [28]. Interestingly, the targets were rather scattered in several clusters, comprising a few targets each and we could not find enrichment in any specific signalling pathway (figure 6c, supplementary figure S15a and b). It thus seems that FGF10 deficiency and cigarette smoke exposure trigger many targets rather than one distinct signalling pathway. However, using such analysis, we could identify clusters related to Wnt signalling in the alveolar wall compartment and tyrosine kinases in the vascular compartment. Along these lines, we found increased Akt phosphorylation and decreased expression of β-catenin in lung homogenates from room air-exposed *Fgf10*$^{+/-}$ and cigarette smoke-exposed wild-type mice (supplementary figure S15c and d).

FGF10 overexpression ameliorates elastase-induced PH and emphysema

As FGF10 overexpression showed a beneficial effect against cigarette smoke-induced emphysema and PH, we next assessed the therapeutic effect of FGF10 in a more severe animal model of elastase-induced emphysema (supplementary figure S16a). Elastase-induced lung injury in mice results in emphysema formation, resembling end-stage emphysema in human patients [10, 29–31]. Intriguingly, FGF10 overexpression completely reversed elastase-induced PH, as shown by the restoration of RVSP, TAPSE and RV mass to the level of healthy controls (figure 7a, supplementary figure S16b and c). Furthermore, FGF10 reversed elastase-induced vascular pruning depicted by pulmonary vasculature casting and von Willebrand factor immunostaining (figure 7b, supplementary figure S16d). In the context of emphysema, FGF10 treatment resulted in a significant repair of the distal lung parenchyma shown as a decrease of lung compliance, elastase-induced increase of airspace and MLI (figure 7c and d, supplementary figure S17a and b). Moreover, design-based stereology analysis revealed increased alveoli density and number in FGF10-treated mice (supplementary figure S17c and d). The number of proliferating (Ki67^{+}) cells was increased in mouse lungs upon FGF10 treatment (supplementary figure S17e). In elastase-induced emphysema, FGF10 overexpression for 1 week caused a significant increase in the number of AT2 cells that gradually returned to baseline (figure 7e), while the area covered by AT1 cells increased (supplementary figure S17f) as the repair process progressed.

FGF10 effect on human COPD lungs

To confirm the relevance of the findings from our animal models for human COPD, we prepared precision-cut lung slices (PCLS) from human COPD lungs. We further cultured them *in vitro* in the presence or the absence of recombinant human FGF10. FGF10 treatment significantly increased the number of proliferating cells, assessed by counting cells that incorporated bromodeoxyuridine (BrdU; BrdU^{+} cells). Most BrdU^{+} cells were located in the alveolar walls, whereas no proliferating cells were found in the tunica media of the pulmonary vasculature (figure 8a). These findings suggest that COPD patients' and mouse lungs retain a regenerative capacity and accordingly respond to FGF10 stimulation. To further explore which cell types respond to FGF10 treatment, we investigated AT2 and endothelial cells in treated PCLS. FGF10 treatment induced an increase in the number/expansion of AT2 and endothelial cells.

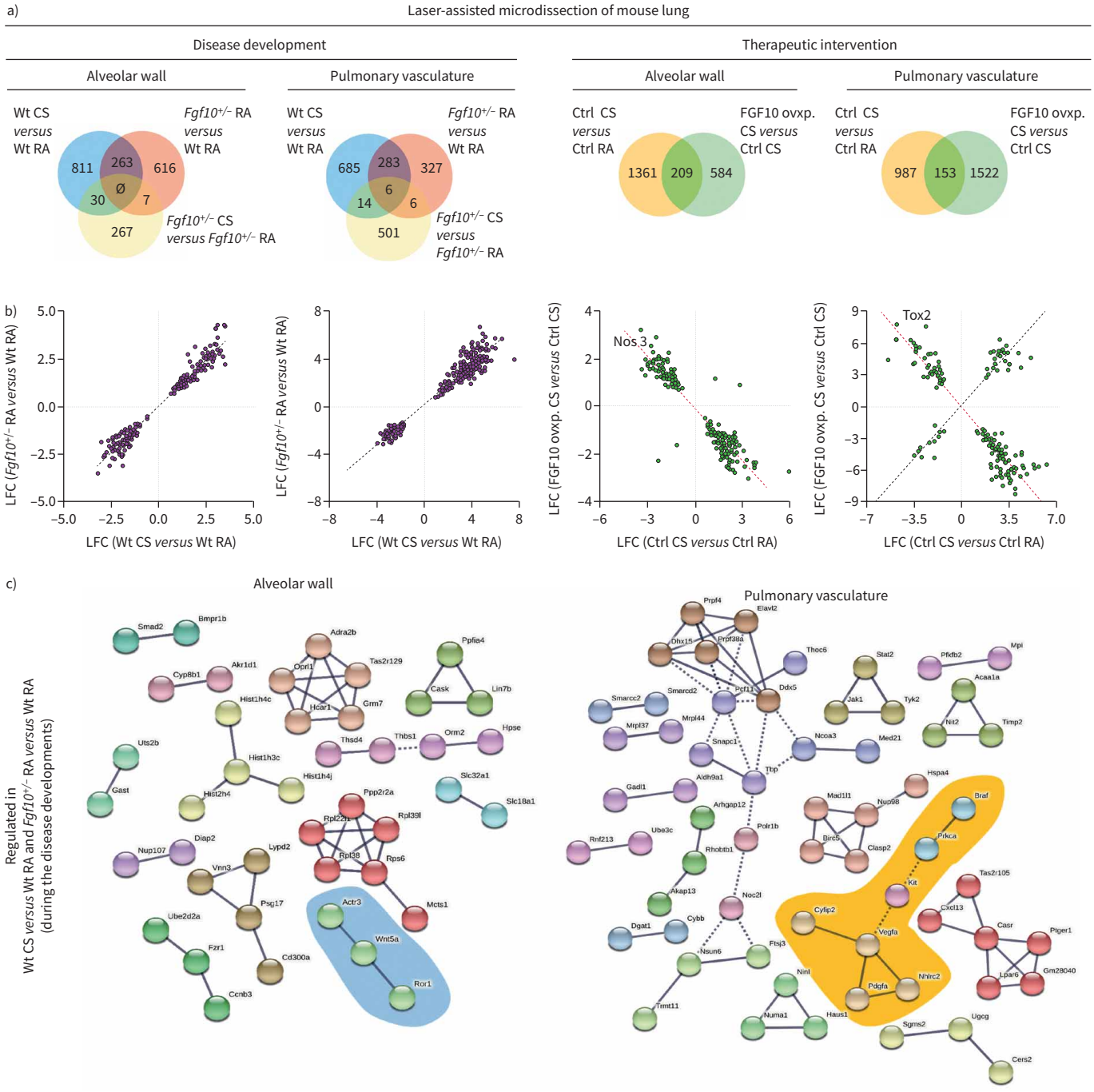

FIGURE 6 Cigarette smoke (CS)- and fibroblast growth factor (FGF)10-related molecular pathways involved in the development or reversion of emphysema and pulmonary hypertension. a) Venn diagrams were used to show the number of dysregulated genes during disease development or therapeutic intervention by FGF10 overexpression in the alveolar wall or the pulmonary vasculature. The overlap regions show genes that are in common for the compared groups. Genes that are commonly regulated (between wild-type (Wt) CS *versus* Wt room air (RA) and *Fgf10*$^{+/-}$ RA *versus* Wt RA during disease development; between control (Ctrl) CS *versus* Ctrl RA and FGF10 overexpression (ovxp) CS *versus* Ctrl CS during the therapeutic intervention) were further investigated. b) Diagrams showing the common genes with the direction of gene expression changes. Between the two compared groups of genes, positive or negative correlation implies the similar or opposite direction of fold changes, respectively. c) Genes that are regulated in Wt CS *versus* Wt RA and *Fgf10*$^{+/-}$ RA *versus* Wt RA during the disease development are investigated using functional protein association networks (STRING-DB). The analysis shows only genes whose products are connected in the alveolar wall compartment or in pulmonary vessels. Genes that play a role in the Wnt signalling pathway and are regulated during the disease development in the alveolar wall compartment are marked in blue. A cluster related to tyrosine kinase signalling in the pulmonary vasculature is marked in orange. Nos3: (endothelial) nitric oxide synthase 3; Ctsk: cathepsin K; Bok: Bcl-2-related ovarian killer; Tox2: TOX high mobility group box family member 2; Wnt5a: Wnt family member 5A; Ror1: receptor tyrosine kinase-like orphan receptor 1; Actr3: actin-related protein 3; Braf: serine/threonine-protein

kinase B rapidly accelerated fibrosarcoma; Prkca: protein kinase Cα; Kit: tyrosine kinase receptor KIT; Vefga: vascular endothelial growth factor A; Cyfip2: cytoplasmic FMR1 interacting protein 2; Nhlrc2: NHL repeat containing 2; Pdgfa: platelet-derived growth factor subunit α; LFC: log fold change.

The FGF10-mediated increase of AT2 cell number had already occurred after 24 h, whereas a significant increase in the number/expansion of endothelial cells was detected after 48 h (figure 8b–d). Moreover, we found an enhanced canonical WNT/β-catenin pathway in FGF10-treated COPD PCLS (figure 8e).

Discussion

In the current study, we provide substantial data that the downregulation of FGF10 correlates with lung emphysema development and severity. Structurally and functionally, our data show that impaired FGF10 signalling in mice leads to spontaneous emphysema and PH development. Transcriptomic analysis revealed that *Fgf10*$^{+/-}$ mice with spontaneous emphysema and PH share the same signalling pathways observed in cigarette smoke-exposed mice. Furthermore, FGF10 overexpression completely reversed established, normally irreversible, emphysema and PH in mice. Thus, FGF10 signalling can be an essential target for the prevention and treatment of, until now, incurable COPD-associated emphysema. The data from our animal models were further validated in human COPD PCLS.

FGF10 expression was decreased in the alveolar wall compartment and increased in the pulmonary vasculature in lung samples explanted from patients with end-stage COPD. In pulmonary vessels of COPD lungs, FGF10 expression was upregulated in the tunica media of proximal muscularised vessels and not regulated in smaller distal vessels. FGF10 is a paracrine factor with limited tissue diffusion [12]. Therefore, the observed FGF10 upregulation in large proximal pulmonary vessels could be insufficient to affect the distal respiratory epithelium and small vessels susceptible to pruning. Similarly, in the lungs of individuals with severe PH, FGF10 expression was increased in vessels, but negatively correlated with disease severity [25], suggesting that FGF10 could play a protective role in the pulmonary vasculature. We detected low circulating FGF10 levels in the serum of COPD patients without correlation with disease severity or PH. FGF10 was downregulated in interstitial COPD lung fibroblasts, and low FGF10 expression in alveolar septal walls was associated with a more severe emphysema phenotype in COPD lungs.

Mice with impaired FGF10 signalling are more prone to develop cigarette smoke-induced emphysema and spontaneously developed emphysema and PH. PH in our transgenic animals is characterised by pulmonary vascular remodelling, shown as an increase in muscularisation of usually nonmuscularised or slightly muscularised small vessels, as previously described in the context of cigarette smoke exposure [4–6, 26]. Besides enhanced kinase signalling that was found in the remodelled vasculature of our experimental mice, endothelial–mesenchymal transition (EMT) could also contribute to muscularisation [32]. Namely, EMT was described as a process contributing to vessel remodelling in mice with impaired FGF signalling in hypoxia-induced PH [32]. However, the contribution of EMT in COPD-associated PH remains obscure [32].

Interestingly, none of the parameters indicating the development of spontaneous emphysema and PH in our transgenic animals worsened upon cigarette smoke exposure, suggesting their saturation. Furthermore, FGF10 expression was decreased in the lung homogenate from cigarette smoke-exposed wild-type mice to the same level as in *Fgf10*$^{+/-}$ mice in room air, and FGF10 expression was not further decreased upon cigarette smoke exposure of *Fgf10*$^{+/-}$ mice. This could explain the lack of further disease worsening in *Fgf10* haploinsufficient mice upon cigarette smoke exposure.

All of our data suggest a similar disease development pattern between cigarette smoke-exposed wild-type and room air-exposed transgenic mice. Furthermore, impaired FGF10 signalling does not only lead to a similar phenotype, but also triggers similar cellular and molecular mechanisms as cigarette smoke-induced emphysema and PH. These mechanisms include increased MMP activity, apoptosis and cellular senescence. Thus, mice with impaired FGF10 signalling may also be used as a genetic animal model of emphysema and PH.

In our animal model, we found β-catenin and Akt pathways to be involved in emphysema and PH development, respectively. Increased Akt phosphorylation could be connected with vascular remodelling [33], senescence [34] and inflammation, described in COPD patients [35]. Furthermore, it has been shown that the WNT/β-catenin pathway is essential for lung development and homeostasis, and it is suggested as a mechanism of lung repair in COPD [8, 36]. However, it appears that both cigarette smoke exposure and FGF10 insufficiency trigger many more similar pathways leading to disease development.

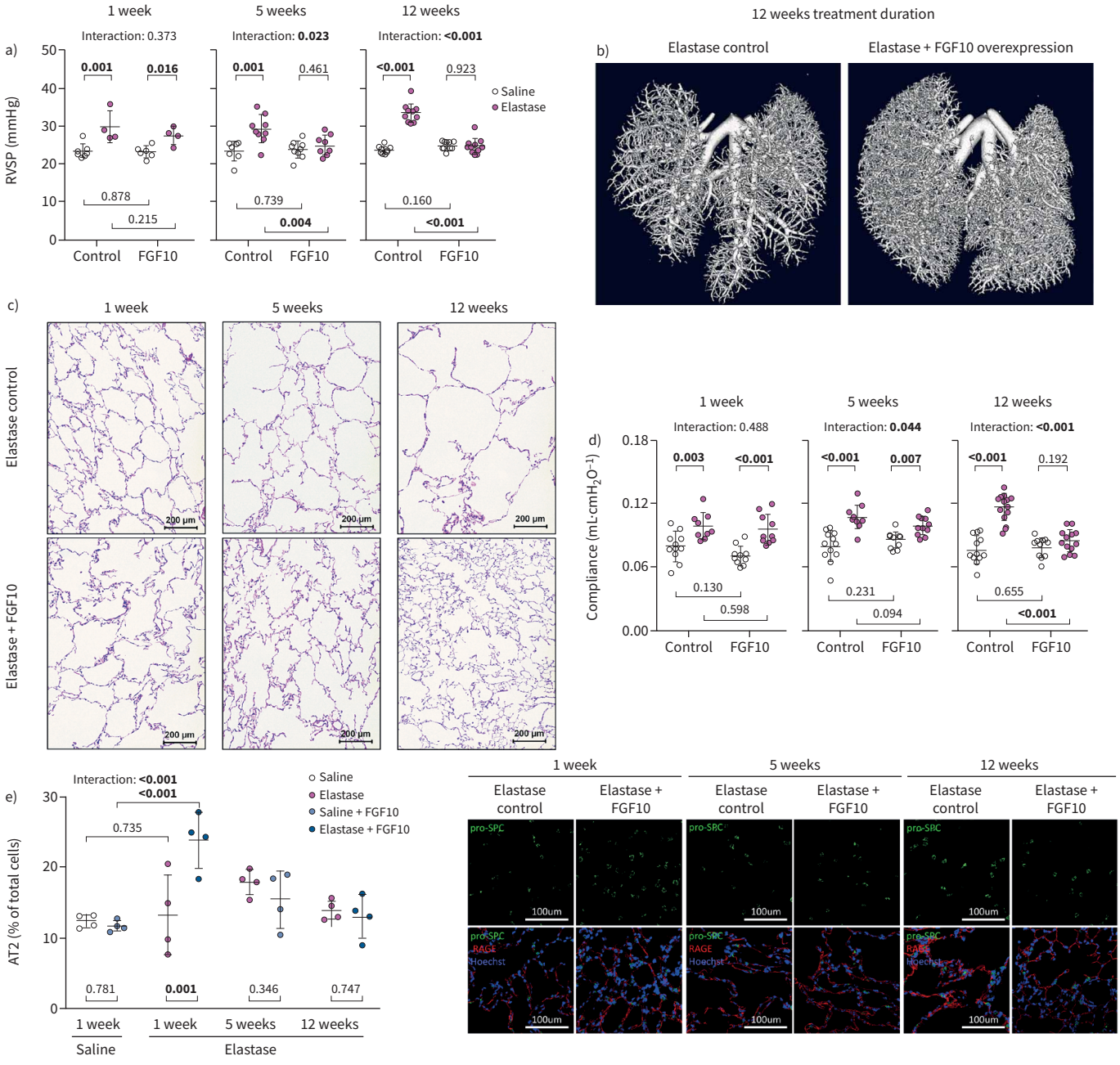

FIGURE 7 Fibroblast growth factor (FGF)10 overexpression ameliorates elastase-induced pulmonary hypertension and emphysema in mice. a) Haemodynamic measurement of the right ventricular systolic pressure (RVSP) (n=4–10) in saline- or elastase-treated mice that were subsequently fed with standard feed (control) or feed containing doxycycline (FGF10) for 1, 5 or 12 weeks. b) Visualisation of the pulmonary vascular tree by *ex vivo* microcomputed tomography scanning in lungs perfused with radiopaque Microfil. c) Representative images of haematoxylin and eosin-stained mouse lung sections after elastase-induced pulmonary emphysema and subsequent treatment by doxycycline-induced FGF10 overexpression for a duration of 1, 5 or 12 weeks. d) *In vivo* lung function measurements showing static lung compliance (n=9–13) in the experimental mice. e) Immunofluorescence staining of markers for alveolar epithelial type 2 cells (AT2, pro-surfactant protein C (pro-SPC)) and type I cells (receptor for advanced glycation end products (RAGE)) in lungs of experimental animals (n=4). Quantification shows percentage of AT2 cells of total lung cells in distal lung parenchyma. No significant changes in nuclei count were detected between analysed groups. In the quantification panels each dot represents a measurement obtained from one individual experimental animal. The mean value for each group is represented by a horizontal line (±SD). Statistical analysis: two-way ANOVA; p-values for each comparison and interaction are given in the graphs. Bold type represents statistical significance.

FGF10 overexpression successfully reversed established cigarette smoke- and elastase-induced emphysema in mice. We show an increase in the alveoli numbers in the lungs of treated animals, which proves that FGF10 treatment, can induce alveologenesis in adult mice with established cigarette smoke- or

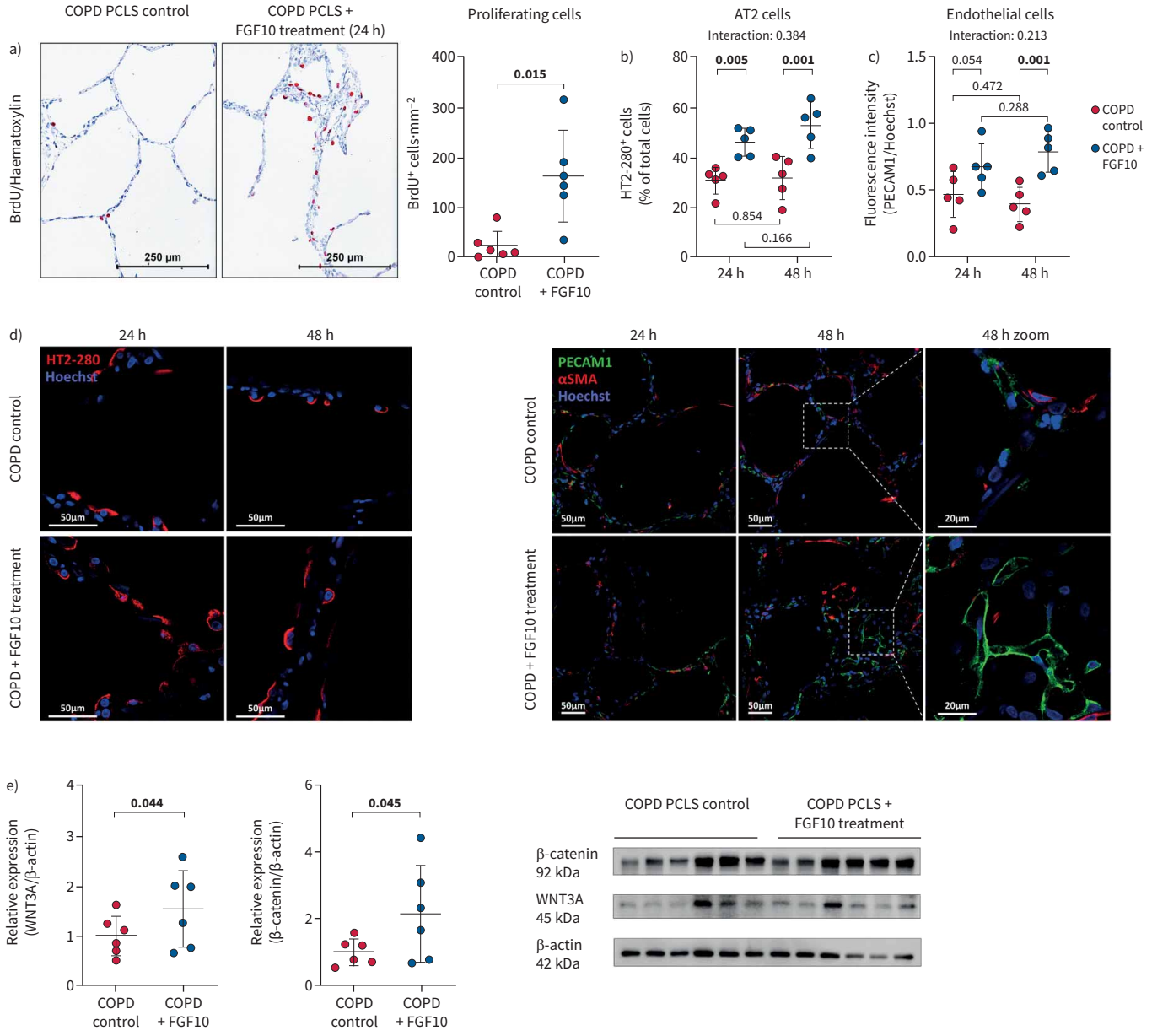

FIGURE 8 Fibroblast growth factor (FGF)10 treatment *in vitro* has beneficial effects on human precision cut lung slices. a) Bromodeoxyuridine-positive ($BrdU^+$) cells in precision-cut lung slices (PCLS) obtained from COPD lungs (n=6) and *in vitro* treated with recombinant human FGF10 for 24 h. Quantification of proliferation shown as the number of $BrdU^+$ cells·mm^{-2} of the analysed tissue area. b–d) Immunostaining and quantification of b) alveolar epithelial type 2 cells (AT2; percentage of HT2–280-positive cells) and c) endothelial cells (platelet and endothelial cell adhesion molecule (PECAM)1 fluorescence intensity) in human COPD PCLS with or without FGF10 treatment at 24 h and 48 h time points (n=5). No significant changes in nuclei count were detected between analysed groups. d) Representative images of immunostaining in PCLS obtained using laser scanning confocal microscopy. e) Protein expression of β-catenin and WNT3A and quantification by densitometry in PCLS homogenates upon 24 h of *in vitro* treatment with recombinant human FGF10 (n=6). In the quantification panels, each dot represents a measurement obtained from one human PCLS (five to six different COPD lungs). Immunohistochemistry: red: BrdU; blue: haematoxylin. The mean value for each group is represented by a horizontal line (±SD). Statistical analysis: a, e) paired t-test; b, c) paired two-way ANOVA; p-values for each comparison and interaction are given in the graphs. Bold type represents statistical significance. αSMA: α-smooth muscle actin.

elastase-induced emphysema. FGF10 overexpression increases epithelial progenitor markers in bronchi and leads to increase in AT2 cell number in distal lung parenchyma before any signs of structural improvement. AT2 cells could be the first responders during the FGF10-mediated emphysema reversion. Interestingly, during the course of the FGF10-mediated alveolar repair in both animal models, the number of AT2 cells returned to the level of healthy controls. The decrease in AT2 cell number suggests their

further differentiation into AT1 cells that can underlie the FGF10-mediated repair of alveolar structures at later time points. We confirmed our data from animal models in human PCLS from COPD patients where FGF10 treatment led to an increase in the number of AT2 cells. Among the regulated pathways, we pinpointed the canonical β-catenin pathway to be downstream of FGF10 treatment in treated mouse lungs and human COPD PCLS.

Furthermore, FGF10 overexpression reversed established cigarette smoke- and elastase-induced PH. Hence, FGF10-mediated reversion of the PH phenotype could rely on the recovery of the capillary network and reversion of pulmonary vascular remodelling.

Taken together, impaired FGF10 signalling can be a molecular mechanism underlying the development of emphysema and PH in COPD. FGF10 overexpression in mice with established emphysema and PH, restored alveolar and vascular structure. Boosting FGF10 signalling may represent a novel treatment concept for lung emphysema and PH in COPD if our findings in mouse models hold true for the human disease. This hypothesis is at least supported by our data from the analysis of the FGF10 pathway in human lung samples, including FGF10 treatment of human PCLS. However, more research is needed regarding adequate application procedures, safety and targeted FGF10 delivery or cell-specific FGF10 pathway stimulation in humans.

Acknowledgements: The authors thank Kerstin Goth, Miriam Wessendorf, Dileep Bonthu, Nils Schupp, Christina Pilz and Karin Quanz for technical assistance; Ingrid Henneke and Thomas Sontag for help with the animal ethical proposals; Marouane Qsaib and Lea Pellekoorne for help with Western blots; and Christine Veith for proofreading (all at Excellence Cluster Cardio-Pulmonary Institute, Universities of Giessen and Marburg Lung Center, Member of the German Center for Lung Research (DZL), Justus-Liebig-University, Giessen, Germany). Portions of the doctoral thesis of Stefan Hadzic are incorporated into this manuscript.

Ethics approval: The ethics committee of the Justus-Liebig-University School of Medicine approved the studies involving human material (AZ 58/15). All animal experiments were approved by the local governmental authorities (Regierungspräsidium Giessen) in accordance with the German animal welfare law and the European legislation for the protection of animals used for scientific purposes (2010/63/EU).

Author contributions: Conceptualisation: S. Hadzic, C-Y. Wu, M. Gredic, O. Pak, M. Seimetz, N. Sommer, D. Kosanovic, D. Warburton, X. Li, E. El Agha, S. Bellusci and N. Weissmann. Methodology: S. Hadzic, C-Y. Wu, M. Gredic, O. Pak, E. Loku, S. Kraut, B. Kojonazarov, J. Wilhelm and M. Brosien. Formal analysis: S. Hadzic, C-Y. Wu, M. Gredic, O. Pak, E. Loku, S. Kraut, B. Kojonazarov, J. Wilhelm, D. Warburton, M. Bendnorz, M. Seimetz, E. El Agha, S. Bellusci and N. Weissmann. Investigation: S. Hadzic, C-Y. Wu, M. Gredic, O. Pak, E. Loku, S. Kraut, B. Kojonazarov, J. Wilhelm, M. Bednorz and M. Seimetz. Resources: M. Seimetz, A. Günther, N. Sommer, F. Grimminger, H.A. Ghofrani, R.T. Schermuly, W. Seeger, S. Bellusci, X. Li and N. Weissmann. Data curation: S. Hadzic, C-Y. Wu, M. Gredic, O. Pak, E. Loku, S. Kraut, B. Kojonazarov, J. Wilhelm, M. Brosien, M. Seimetz, E. El Agha, S. Bellusci and N. Weissmann. Writing (original draft): S. Hadzic, C-Y. Wu, O. Pak, J. Wilhelm, E. El Agha, S. Bellusci and N. Weissmann. Visualisation: S. Hadzic, C-Y. Wu, M. Gredic, O. Pak, B. Kojonazarov, E. El Agha, S. Bellusci and N. Weissmann. Supervision: O. Pak, D. Kosanovic, M. Seimetz, N. Sommer, R.T. Schermuly, W. Seeger, S. Bellusci and N. Weissmann. Project administration: S. Hadzic, M. Brosien, M. Seimetz, A. Günther, N. Sommer, F. Grimminger, H.A. Ghofrani, R.T. Schermuly, W. Seeger, S. Bellusci and N. Weissmann. Funding acquisition: M. Seimetz, N. Sommer, F. Grimminger, H.A. Ghofrani, R.T. Schermuly, W. Seeger, S. Bellusci and N. Weissmann.

Conflict of interest: The authors have no potential conflicts of interest to disclose.

Support statement: This work was supported by the German Research Foundation (DFG; BE 4443/6-1; project ID 268555672, SFB 1213: A04, A06, A07, CP02; KFO309: P7), as well as the Excellence Cluster Cardio-Pulmonary Institute (CPI). Funding information for this article has been deposited with the Crossref Funder Registry.

References

1 Barnes PJ, Burney PGJ, Silverman EK, *et al.* Chronic obstructive pulmonary disease. *Nat Rev Dis Primers* 2015; 1: 15076.
2 Barnes PJ. Cellular and molecular mechanisms of chronic obstructive pulmonary disease. *Clin Chest Med* 2014; 35: 71–86.
3 Hadzic S, Wu CY, Avdeev S, *et al.* Lung epithelium damage in COPD – an unstoppable pathological event? *Cell Signal* 2020; 68: 109540.

4 Gredic M, Blanco I, Kovacs G, *et al.* Pulmonary hypertension in chronic obstructive pulmonary disease. *Br J Pharmacol* 2021; 178: 132–151.
5 Pichl A, Sommer N, Bednorz M, *et al.* Riociguat for treatment of pulmonary hypertension in COPD: a translational study. *Eur Respir J* 2019; 53: 1802445.
6 Seimetz M, Parajuli N, Pichl A, *et al.* Inducible NOS inhibition reverses tobacco-smoke-induced emphysema and pulmonary hypertension in mice. *Cell* 2011; 147: 293–305.
7 Peinado VI, Pizarro S, Barberà JA. Pulmonary vascular involvement in COPD. *Chest* 2008; 134: 808–814.
8 Kruk D, Wisman M, de Bruin HG, *et al.* Abnormalities in reparative function of lung-derived mesenchymal stromal cells in emphysema. *Am J Physiol Lung Cell Mol Physiol* 2021; 320: L832–L844.
9 Kojonazarov B, Hadzic S, Ghofrani HA, *et al.* Severe emphysema in the SU5416/hypoxia rat model of pulmonary hypertension. *Am J Respir Crit Care Med* 2019; 200: 515–518.
10 Yildirim AO, Muyal V, John G, *et al.* Palifermin induces alveolar maintenance programs in emphysematous mice. *Am J Respir Crit Care Med* 2010; 181: 705–717.
11 Klar J, Blomstrand P, Brunmark C, *et al.* Fibroblast growth factor 10 haploinsufficiency causes chronic obstructive pulmonary disease. *J Med Genet* 2011; 48: 705–709.
12 Ornitz DM, Itoh N. The fibroblast growth factor signaling pathway. *Wiley Interdiscip Rev Dev Biol* 2015; 4: 215–266.
13 Bellusci S, Grindley J, Emoto H, *et al.* Fibroblast growth factor 10 (FGF10) and branching morphogenesis in the embryonic mouse lung. *Development* 1997; 124: 4867–4878.
14 Yuan T, Volckaert T, Redente EF, *et al.* FGF10-FGFR2B signaling generates basal cells and drives alveolar epithelial regeneration by bronchial epithelial stem cells after lung injury. *Stem Cell Reports* 2019; 12: 1041–1055.
15 Gupte VV, Ramasamy SK, Reddy R, *et al.* Overexpression of fibroblast growth factor-10 during both inflammatory and fibrotic phases attenuates bleomycin-induced pulmonary fibrosis in mice. *Am J Respir Crit Care Med* 2009; 180: 424–436.
16 Ahmadvand N, Khosravi F, Lingampally A, *et al.* Identification of a novel subset of alveolar type 2 cells enriched in PD-L1 and expanded following pneumonectomy. *Eur Respir J* 2021; 58: 2004168.
17 Volckaert T, Dill E, Campbell A, *et al.* Parabronchial smooth muscle constitutes an airway epithelial stem cell niche in the mouse lung after injury. *J Clin Invest* 2011; 121: 4409–4419.
18 Volckaert T, Yuan T, Chao CM, *et al.* Fgf10-Hippo epithelial-mesenchymal crosstalk maintains and recruits lung basal stem cells. *Dev Cell* 2017; 43: 48–59.
19 Moiseenko A, Vazquez-Armendariz AI, Kheirollahi V, *et al.* Identification of a repair-supportive mesenchymal cell population during airway epithelial regeneration. *Cell Rep* 2020; 33: 108549.
20 Jackson VE, Latourelle JC, Wain LV, *et al.* Meta-analysis of exome array data identifies six novel genetic loci for lung function. *Wellcome Open Res* 2018; 3: 4.
21 Smith BM, Traboulsi H, Austin JHM, *et al.* Human airway branch variation and chronic obstructive pulmonary disease. *Proc Natl Acad Sci USA* 2018; 115: E974–E981.
22 Hadzic S, Wu CY, Gredic M, *et al.* The effect of long-term doxycycline treatment in a mouse model of cigarette smoke-induced emphysema and pulmonary hypertension. *Am J Physiol Lung Cell Mol Physiol* 2021; 320: L903–L915.
23 Diaz AA, Maselli DJ, Rahaghi F, *et al*. Pulmonary vascular pruning in smokers with bronchiectasis. *ERJ Open Res* 2018; 4: 00044–2018.
24 Jones MR, Chong L, Bellusci S. Fgf10/Fgfr2b signaling orchestrates the symphony of molecular, cellular, and physical processes required for harmonious airway branching morphogenesis. *Front Cell Dev Biol* 2021; 8: 44.
25 El Agha E, Schwind F, Ruppert C, *et al*. Is the fibroblast growth factor signaling pathway a victim of receptor tyrosine kinase inhibition in pulmonary parenchymal and vascular remodeling? *Am J Physiol Lung Cell Mol Physiol* 2018; 315: L248–L252.
26 Seimetz M, Sommer N, Bednorz M, *et al.* NADPH oxidase subunit NOXO1 is a target for emphysema treatment in COPD. *Nat Metab* 2020; 2: 532–546.
27 Basson J, Sung YJ, Schwander K, *et al.* Gene-education interactions identify novel blood pressure loci in the Framingham Heart Study. *Am J Hypertens* 2014; 27: 431–444.
28 Szklarczyk D, Gable AL, Lyon D, *et al.* STRING v11: protein–protein association networks with increased coverage, supporting functional discovery in genome-wide experimental datasets. *Nucleic Acids Res* 2019; 47: D607–D613.
29 Fysikopoulos A, Seimetz M, Hadzic S, *et al.* Amelioration of elastase-induced lung emphysema and reversal of pulmonary hypertension by pharmacological iNOS inhibition in mice. *Br J Pharmacol* 2021; 178: 152–171.
30 Antunes MA, Rocco PR. Elastase-induced pulmonary emphysema: insights from experimental models. *An Acad Bras Cienc* 2011; 83: 1385–1396.
31 Limjunyawong N, Craig JM, Lagassé HA, *et al.* Experimental progressive emphysema in BALB/cJ mice as a model for chronic alveolar destruction in humans. *Am J Physiol Lung Cell Mol Physiol* 2015; 309: L662–L676.

32 Woo KV, Shen IY, Weinheimer CJ, *et al.* Endothelial FGF signaling is protective in hypoxia-induced pulmonary hypertension. *J Clin Invest* 2021; 131: e141467.

33 Tang H, Chen J, Fraidenburg DR, *et al.* Deficiency of Akt1, but not Akt2, attenuates the development of pulmonary hypertension. *Am J Physiol Lung Cell Mol Physiol* 2015; 308: L208–L220.

34 Houssaini A, Breau M, Kebe K, *et al.* mTOR pathway activation drives lung cell senescence and emphysema. *JCI Insight* 2018; 3: e93203.

35 Bozinovski S, Vlahos R, Hansen M, *et al.* Akt in the pathogenesis of COPD. *Int J Chron Obstruct Pulmon Dis* 2006; 1: 31–38.

36 Conlon TM, John-Schuster G, Heide D, *et al.* Inhibition of LTβR signalling activates WNT-induced regeneration in lung. *Nature* 2020; 588: 151–156.